

Corrosion Inhibition of Steel in Dense Supercritical CO₂ with Sulfurous Acid Impurity

Meng Ma^{1,2}, Yong Xiang^{1,3,*}, Chen Li^{1,3}, Jiangyun Wang⁴, Laibin Zhang¹

¹*College of Mechanical and Transportation Engineering, China University of Petroleum, Beijing, 102249 P.R. China, xiangy03@foxmail.com*

²*Technology Inspection Center of Shengli Oilfield Branch, SINOPEC Corp., Dongying, 257000 P.R. China*

³*Beijing Key Laboratory of Process Fluid Filtration and Separation, China University of Petroleum, Beijing 102249 P.R. China*

⁴*College of Chemical Engineering, China University of Petroleum, Beijing 102249, P.R. China*

Abstract

Corrosion inhibition of steel in dense supercritical CO₂ with impurities is a newly generated issue concerned with carbon capture and storage (CCS). Based on the experiment results in the current work, the issue of steel corrosion inhibition in dense supercritical CO₂ environments with sulfurous acid impurity was investigated and discussed. The experiment results indicated that the Clariant inhibitor 793, 794 and imidazoline-based inhibitor K₁ did not show much inhibition effect. It seems like that the diffusion ability of inhibitors in supercritical CO₂ was weak or the inhibitors were not soluble in supercritical CO₂ phase, so it might result in that the steel sample surface was not covered by the inhibitors. Supercritical CO₂ soluble inhibitor is urgently needed in order to effectively reduce the corrosion rate of steel in dense supercritical CO₂ environments with kinds of acid gas impurities for CCS purpose.

Keywords: CCS, supercritical CO₂, inhibitor, soluble, acid gas impurity.

Introduction

Corrosion of steel in dense supercritical CO₂ is one of the hottest research topics in corrosion science research society due to the continuously increasing attentions of human beings to the global climate change and carbon capture and storage (CCS), and the latter is supposed to be the most effective way to address the global climate change problem. It has been confirmed that when the dense supercritical CO₂ is transported in the pipeline mixed with acid gas impurities (SO_x, NO_x, H₂S, HCl) and H₂O, the corrosion rate of pipeline steel will greatly increase due to the formation of strong acids [1–4], which can provide a bunch

of H^+ ions to participate in the cathodic reaction of corrosion process. It was reported that 2 ppmw of HCl contamination in supercritical CO_2 can cause a decrease of pH to less than 1.5 [5]. SO_x and NO_x can also form sulfuric acid and nitric acid, which can also decrease the pH of the condensates dramatically. The synergistic effect of these acid impurities on the pH and corrosion is more notable and complex, and their corrosion mechanisms are not clear.

If water can be easily and economically removed, then the problem can be solved immediately, because many experimental study results [6–10] and the field experiences of CO_2 pipeline transport in USA [11] and China Shengli Oilfield have shown that, when CO_2 was water free or low moisture content, the corrosion rates of inner pipeline steel were zero or relatively low. If dehydration and the other impurity purification processes are low cost, any research issues related to the inner corrosion of CO_2 pipeline make no sense. The fact is that the related corrosion research is in the ascendant, and the dehydration process is not cheap [12, 13]. High cost is the main reason for the restriction of CCS developed in large scale.

Using corrosion resistant alloys (CRAs) might be another choice to address this corrosion problem. However, the huge investment of the pipeline construction should be the barrier to choose this way, especially for the large-scale scenario of CCS in the future. Also, the suitable CRAs for supercritical CO_2 transport with acid gas impurities have not been properly selected yet.

Employing Inhibitors to control CO_2 corrosion in the oil and gas industry has long history. The performance of kinds of inhibitor in the CO_2 -saturated solution has been widely studied [14–18]. However, these studies were usually under low CO_2 partial conditions. Imidazoline-based inhibitors are the mostly used inhibitors in oil and gas field to control the CO_2 corrosion. When these inhibitors are used to dense supercritical CO_2 environments, the performance of these inhibitors might be unreliable and inefficient [19]. When the water soluble or volatile inhibitors are used in dense supercritical CO_2 environments, the solubility and diffusion coefficients of the inhibitors might have great difference with the cases when they are in the liquid or gas phase. Whether these inhibitors can reach the steel surface and form the stable film to protect the substrate metal is questionable when these inhibitors are placed in dense supercritical CO_2 phase. Whether there is an inhibitor that can withstand the attack of kinds of acid gas impurities in dense supercritical CO_2 phase is also questionable.

Currently, there are few open literatures devoted on this issue. The performance of several inhibitors in supercritical CO_2 -saturated solution was tested by Zhang et al., while the

performance of inhibitors in water-saturated supercritical CO₂ was not addressed [20]. Marks et al. investigated the impacts of Mn-Mg based zinc phosphate and vanadate used as the corrosion inhibition method in dense supercritical CO₂ for the CCS purpose [21]. The high inhibition efficiency was achieved when the pH was at 4, while the experiment results also indicated that the inhibition efficiency was pretty low when pH of the solution was further lowered to the region of 1–3.

In the present work, three inhibitors were tested in dense supercritical CO₂ environment with sulfurous acid impurity, including Clariant inhibitor 793, 794 and imidazoline-based inhibitor K₁. Sulfurous acid was added as the possible impurity in the CCS CO₂ pipeline, simulating the situation with SO₂ and H₂O impurities. The weight-loss method was used to evaluate the inhibition efficiency of the inhibitors. Scanning electron microscopy (SEM), energy dispersive X-ray spectroscopy (EDS), X-ray diffraction (XRD) and Raman spectroscopy were employed to investigate the surface morphology, chemical and the phase compositions of the corroded samples, respectively. The results were discussed and the research needs were also pointed out for the further investigation.

Materials and methods

Test samples were machined from API 5L X65 pipeline steel. The elemental composition of the used steel was listed in Table 1. The sample used for weight-loss method had a size of 50×25×3 mm, while the sample used for SEM/EDS, XRD and Raman had a size of 10×10×1 mm. Corrosion inhibitor experiments were performed in a 7.5 L hastelloy autoclave (Cortest, USA). The Clariant inhibitor 793 and 794 are the inhibitor that Clariant Corporation specially developed for the inhibition of internal pipeline corrosion of CCS which may contain SO₂ impurity. For the business secret, the compositions of the inhibitors are not listed in this paper.

Before each test, the samples were polished with silicon carbide (SiC) paper progressively up to 600 grit, cleaned with isopropyl alcohol (C₃H₈O) in an ultrasonic bath, dried, and weighed using an electronic balance with a precision of 0.01 mg. Four samples were placed inside the autoclave for each test and three samples were for the weight-loss method. N₂ was pumped into the autoclave for 2 h to remove the oxygen in the autoclave before each test. Then, 187.5 ml sulfurous acid (containing 6.0% H₂SO₃ by weight) and 100 ppm (0.75 ml) or 400 ppmv (3.0 ml) inhibitor were added into the autoclave bottom. Once the autoclave was sealed, temperature was adjusted. Finally, high pressure CO₂ was added into the autoclave with a gas booster pump to the desired working pressure. Details of the experimental conditions are given in Table 2.

The weight-loss method was used to calculate the average corrosion rate for three samples in each test, which were exposed simultaneously to the corrosion environments. After each test, the samples were cleaned using the Clarke solution (20 g Sb₂O₃ and 50 g SnCl₂ and concentrated hydrochloric acid to make 1000 ml) [22], rinsed with de-ionized water, dried, and weighed by the electronic balance. The average corrosion rate can be calculated by the following equation [23]:

$$CR = 8.76 \times 10^4 \frac{\Delta m}{\rho \cdot S \cdot t} \quad (1)$$

where, CR is the corrosion rate, mm/year (mm/y); Δm is the weight loss of the sample, g; ρ is the density of the specimen, g/cm³; S is the area of the sample, cm²; t is the immersion time, h.

Table 1: Elemental composition of the API 5L X65 steel (wt%)

C	Mn	Si	P	S	Cu	Cr	Ni	Al	Mo	Fe
0.065	1.54	0.25	0.013	0.001	0.04	0.05	0.04	0.041	0.007	Balance

The inhibition efficiency was calculated by applying the following formula [21]:

$$\eta(\%) = \frac{W_u - W_i}{W_u} \times 100 \quad (2)$$

where η is the inhibition efficiency, W_u and W_i are the average weight loss of test samples after immersed in dense supercritical CO₂ without and with inhibitor, respectively. The morphology and compositions of the corroded small samples were analyzed with SEM/EDS, XRD, and Raman techniques.

Table 2: Test matrix for the corrosion inhibitor experiments

Test No.	Temperature (K)	Pressure (MPa)	Sulfurous acid (ml)	Immersion time (h)	Inhibitor type	Inhibitor concentration (ppmv)
1	323	8.0	187.5	24	–	–
2	323	8.0	187.5	2	793	100
3	323	8.0	187.5	24	793	100
4	323	8.0	187.5	24	793	400
5	323	8.0	187.5	24	794	400
6	323	8.0	187.5	24	K ₁	400

Results and discussion

Weight-loss results

The weight-loss results for different test conditions were illustrated in Figure 1. The case with 400 ppmv inhibitor 794 had an inhibition efficiency of 13.1%, while the case with 400 ppmv inhibitor K_1 had an inhibition efficiency of 5.0%, which can also be ignored considering the system error of the experiments. The cases with 100 and 400 ppmv inhibitor 793 immersed for 24 h had higher corrosion rates compared with the blank test. For the 2 h test with 100 ppmv inhibitor 793, the corrosion rate was higher than all cases immersed for 24 h, even for the case with higher inhibitor concentration. It has been confirmed by Xiang et al. [24] that the corrosion rate of carbon steel in supercritical CO_2 with SO_2 impurity decreased with the immersion time, especially for the initial few hours. The accumulation of corrosion product scales acting as the barrier between aggressive media and the base metal.

It can be concluded that all the three inhibitors tested have no obvious corrosion inhibition effect in dense supercritical CO_2 with sulfurous acid impurity. The most possible reason for this result is that the inhibitors did not reach the inhibitor surface enough to block corrosion.

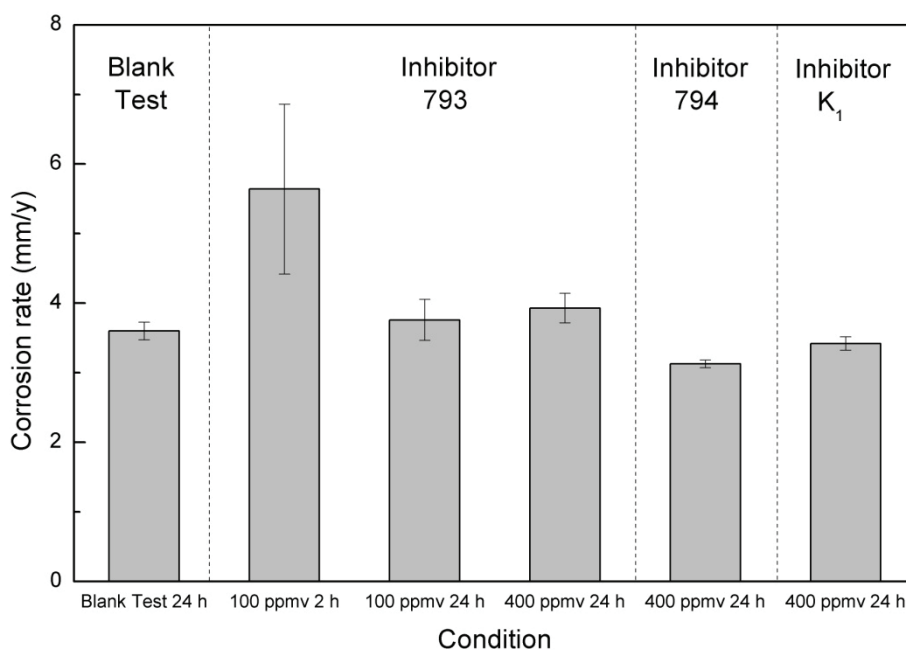


Figure 1: Weight-loss results for different test conditions.

Morphology analysis

The surface morphology SEM images of corroded samples were shown in Figure 2. Many flower shaped corrosion products were found on the corroded sample surface for all the cases exposed for 24 h. In the flower shaped corrosion products, there were many strip shaped corrosion products piled up in a very regular arrangement, which have also been found in tests by other researchers [2, 4]. For the case exposed for 2 h, there were many cracks on the sample surface, which was similar with the surface morphology of the X70 steel sample corroded in dense supercritical $\text{CO}_2/\text{SO}_2/\text{O}_2/\text{H}_2\text{O}$ with a relative humidity of 50% immersed for 120 h [8]. It seems like that the inhibitors had no obvious impact on the surface morphology of the corroded samples, which might indirectly indicate that the corrosion inhibition effect of these inhibitors were weak in dense supercritical CO_2 with sulfurous acid impurity.

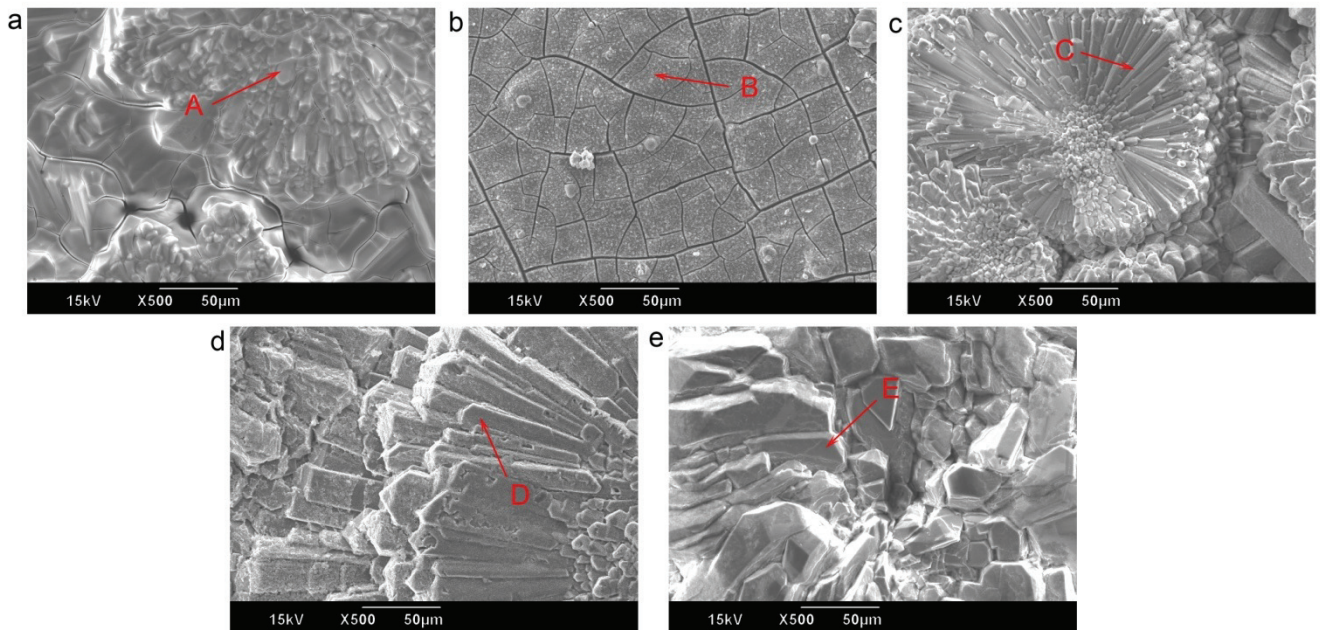


Figure 2: Surface morphology of corroded samples for different test conditions. (a) Blank test, 24 h; (b) 100 ppmv inhibitor 793, 2 h; (c) 100 ppmv inhibitor 793, 24 h; (d) 400 ppmv inhibitor 793, 24 h; (e) 400 ppmv inhibitor 794, 24 h.

The elemental compositions of marked regions A to E based on the EDS detection results were shown in Table 3. For all the cases, Fe, S, and O were detected as the main elemental compositions of the corrosion products. Element carbon was detected for most of the cases, while Si was only found in region B, which came from the original steel composition.

Table 3: Elemental compositions of marked regions (mol%).

Region	Fe	S	O	C	Si
A	15.99	18.45	50.78	14.79	–
B	22.38	20.79	44.07	11.85	0.92
C	22.53	24.78	52.69	–	–
D	18.95	20.96	46.16	13.93	–
E	19.23	20.45	47.93	12.39	–

The surface morphology of corroded samples after removal of scales for the case with 400 ppmv inhibitor 794 exposed for 24 h was illustrated in Figure 3. It can be observed from the SEM image that the surface of the sample was uneven, which might indicate the occurrence possibility of further localized corrosion. The occurrence of localized corrosion of carbon steel in supercritical CO₂ with SO₂, O₂ and H₂O impurities has been confirmed by many studies [6, 25, 26].

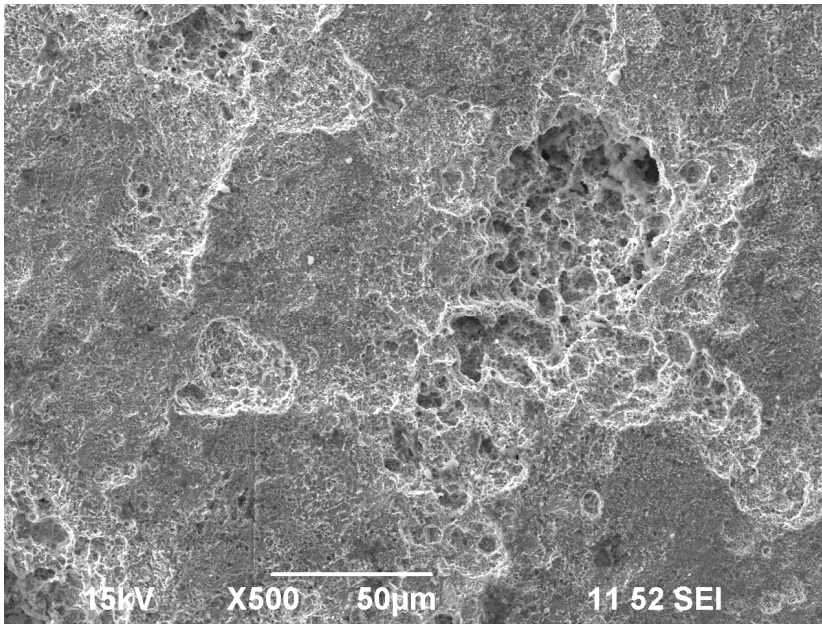
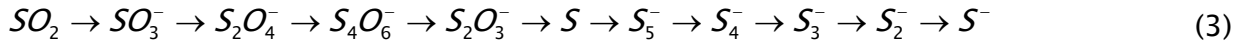


Figure 3. Surface morphology of corroded samples after removal of product scales (400 ppmv inhibitor 794, 24 h).

XRD and Raman analysis

The XRD spectra of the blank test sample were shown in Figure 4. Rozenite (FeSO₄·4H₂O), ferrous sulfite hydrate (FeSO₃·3H₂O), and pyrrhotite (Fe₇S₈) were detected as the main composition of the corrosion products. Rozenite and ferrous sulfite were the common

corrosion products when SO_2 and O_2 exist in wet supercritical CO_2 [2, 4], while pyrrhotite (Fe_7S_8) was seldom found in the corrosion product in that environment. It has to be mentioned that oxygen was not present in the current study for all the tests. Under anaerobic condition, SO_2 might change into sulphur or sulphide through several steps as follows [27]:



The similar case was also found by Ruhl and Kranzmann that the inner part of the $\text{FeSO}_3 \cdot x\text{H}_2\text{O}$ and $\text{FeSO}_4 \cdot x\text{H}_2\text{O}$ corrosion product scales might have changed into iron sulfide [28], for the inner part of the product scales might be under anaerobic condition due to the blocking effect of scales to oxygen.

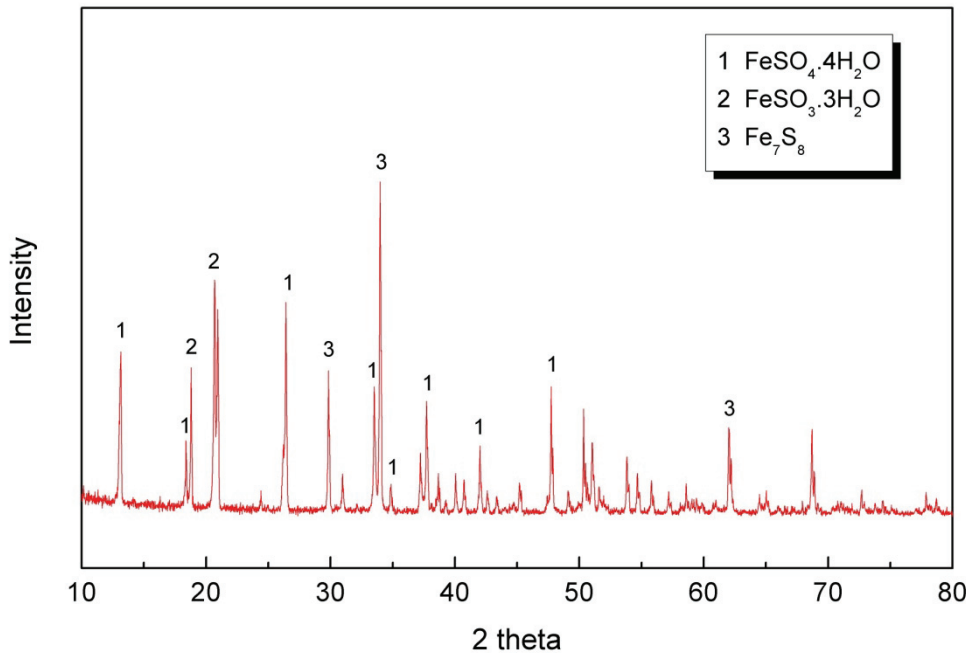


Figure 4: XRD spectra of corroded sample for the blank test.

The Raman spectra of the corroded sample exposed in supercritical CO_2 with sulfurous acid impurity and 100 ppmv inhibitor 793 exposed for 24 h were illustrated in Figure 5. The peak at 219.5, 280, and 388.5 cm^{-1} should indicate the existence of pyrrhotite [29]. The results of these Raman spectra were unable to show the existence of iron sulfate and sulfite in the corrosion products. The Raman spectra also revealed no information of possible residual inhibitor 793 on the corroded sample surface.

It has to be mentioned that the traditional CO_2 corrosion product siderite (FeCO_3) was not found in the current tests. The simple reason is that if siderite forms, it will be dissolved by the sulfurous acid.

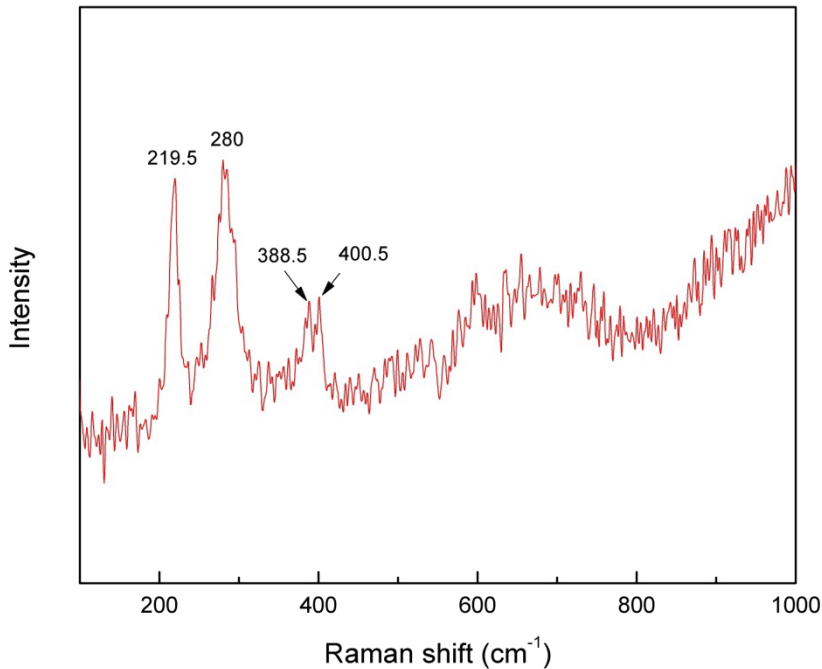


Figure 5: Raman spectra of the corroded sample exposed in supercritical CO_2 with sulfurous acid impurity and 100 ppmv inhibitor 793 for 24 h.

General discussion

All the three inhibitors tested in the current study were verified that they had no notable corrosion inhibition effect on the X65 steel in dense supercritical CO_2 with sulfurous acid impurity.

According to the experimental data by Bamberger et al. [30], the solubility of H_2O in supercritical CO_2 is 3400 mol ppm under the experimental conditions of the present study. Since 187.5 mL sulfurous acid was added into the autoclave for each test, only a small part of water (2.3 g) coming from the sulfurous acid dissolved in dense supercritical CO_2 , the left water formed a separated condensed phase, which contained the dissolved CO_2 and sulfurous acid, and also contained the dissolved inhibitor. The test results possibly indicated that inhibitors were mostly dissolved in the condensed phase, rather than in the supercritical CO_2 phase. If partition coefficient of inhibitor is defined as the ratio of

concentration of inhibitor in supercritical CO₂ phase and in the condensed liquid phase, the partition coefficient should be small.

Another issue that has to be discussed here is the diffusion coefficient of the inhibitor in the supercritical CO₂ phase. Like the rate controlling step concept, if the diffusion process becomes to be the barrier of the inhibitor reaching the steel sample surface, it can also make the inhibitor lose the corrosion inhibition effect due to insufficient inhibitor on the steel surface. The phase of CO₂ in the pipeline may also change into liquid phase, so the solubility and diffusion coefficient of the inhibitors should also be notable in liquid CO₂.

It has been mentioned by Sim et al. that there is no typical common inhibitor to protect steel at low pH, and it is not yet known that such an inhibitor may exist which can function in competition with carbonate scale formation in supercritical conditions [31]. It is also not sure that whether there is an inhibitor that can withstand the attack of kinds of acid gas impurities, such as SO_x, NO_x, HCl, and H₂S. The synergistic effect of these acid gas impurities on and corrosion process is complex.

More researches are needed to be done by the inhibitor scientists and engineers. The need of synthesis and selecting effective inhibitors to inhibit the internal pipeline corrosion of transported dense supercritical CO₂ with kinds of acid gas impurities is urgent. If this way does not work effectively, removing water or using the CRAs as the pipeline materials should be reconsidered seriously.

Conclusions

Three possible inhibitors that might be used in dense supercritical CO₂ with sulfurous acid impurity to inhibit the corrosion of pipeline steel were tested for different immersion time and concentration conditions. The following conclusions can be given:

- The inhibition effects of these inhibitors were all weak. The case with 400 ppmv inhibitor 794 had an inhibition efficiency of 13.1%, while the case with 400 ppmv inhibitor K₁ had an inhibition efficiency of 5.0%, which can also be ignored considering the system error of the experiments.
- Iron sulfate, sulfite and sulfide were found as the main composition of the corrosion products. When O₂ is absent in SO₂ containing environment, iron sulfide may form through several steps.

- Supercritical CO₂ soluble inhibitor is needed, and it also should have the ability to protect the carbon steel under dense supercritical CO₂ environments with kinds of acid gas impurities. If this does not work effectively, removing water or using the CRAs as the pipeline materials should be reconsidered as the corrosion control strategy of supercritical CO₂ pipeline in CCS scenario.

Acknowledgements

This work received financial support by Science Foundation of China University of Petroleum, Beijing, China (No. 2462014YJRC043 and 2462015YQ0402).

References

- [1] 'Effect of liquid impurities on corrosion of carbon steel in supercritical CO₂', F. Ayello, N. Sridhar, K. Evans, R. Thodla, in: Proceedings of the 8th International Pipeline Conference (IPC2010), Calgary, Alberta, Canada, 2010.
- [2] 'Effect of Impurities on the Corrosion Behavior of CO₂ Transmission Pipeline Steel in Supercritical CO₂-Water Environments', Y.S. Choi, S. Nesic, D. Young, *Environmental Science & Technology*, 44, 23, pp9233–9238, 2010.
- [3] 'Experimental techniques used for corrosion testing in dense phase CO₂ with flue gas impurities', A. Dugstad, M. Halseid, B. Morland, in: CORROSION/2014, San Antonio, Texas, USA. Paper No. 4383, 2014.
- [4] 'Impact of SO₂ concentration on the corrosion rate of X70 steel and iron in water-saturated supercritical CO₂ mixed with SO₂', Y. Xiang, Z. Wang, C. Xu, C. Zhou, Z. Li, W. Ni, *The Journal of Supercritical Fluids*, 58, 2, pp286–294, 2011.
- [5] 'State of the aqueous phase in liquid and supercritical CO₂ as relevant to CCS pipelines', I.S. Cole, D.A. Paterson, P. Corrigan, S. Sim, N. Birbilis, *International Journal of Greenhouse Gas Control*, 7, pp82–88, 2012.
- [6] 'The influence of SO₂ on the tolerable water content to avoid pipeline corrosion during the transportation of supercritical CO₂', Y. Hua, R. Barker, A. Neville, *International Journal of Greenhouse Gas Control*, 37, pp412–423, 2015.
- [7] 'Effect of supercritical carbon dioxide (CO₂) on construction materials', F.W. Schremp, G.R. Roberson, *SPE Journal*, 15, 3, pp227–233, 1975.

- [8] 'The upper limit for moisture content in CO₂ pipeline transport', Y. Xiang, Z. Wang, X. Yang, Z. Li, W. Ni, *The Journal of Supercritical Fluids*, 67, pp14–21, 2012.
- [9] 'Water impact on corrosion resistance of pipeline steels in circulating supercritical CO₂ with SO₂– and NO₂– impurities', O. Yevtushenko, R. Bäßler, in: CORROSION/2014, NACE International, San Antonio, TX, USA, Paper No. 3838, 2014.
- [10] 'Water effect on steel under supercritical CO₂ condition', Y. Zhang, K. Gao, G. Schmitt, in: CORROSION/2011, NACE International, Houston, TX, USA, Paper No. 11378, 2011.
- [11] 'Dynamis CO₂ quality recommendations', E. de Visser, C. Hendriks, M. Barrio, M.J. Molnvik, G. de Koeijer, S. Liljemark, Y. Le Gallo, *International Journal of Greenhouse Gas Control*, 2, 4, pp478–484, 2008.
- [12] 'CO₂ purification. Part II: Techno-economic evaluation of oxygen and water deep removal processes', Z. Abbas, T. Mezher, M.R.M. Abu-Zahra, *International Journal of Greenhouse Gas Control*, 16, pp335–341, 2013.
- [13] 'CO₂ purification. Part I: Purification requirement review and the selection of impurities deep removal technologies', Z. Abbas, T. Mezher, M.R.M. Abu-Zahra, *International Journal of Greenhouse Gas Control*, 16, pp324–334, 2013.
- [14] 'Research on the CO₂ corrosion inhibitor technology in Oil and gas fields', Y. Cheng, Z. Li, H. Bi, Y. Song, in: J. Wu, X. Lu, H. Xu, N. Nakagoshi (Eds.) *Resources and Sustainable Development*, Pts 1–4, 2013, pp. 1240–1245.
- [15] 'Corrosion inhibitors performance for mild steel in CO₂ containing solutions', G.Z. Olivares, M.J.H. Gayosso, J.L.M. Mendoza, *Materials and Corrosion–Werkstoffe Und Korrosion*, 58, 6, pp427–437, 2007.
- [16] 'CO₂ corrosion control in steel pipelines. Influence of turbulent flow on the performance of corrosion inhibitors', M. Elena Olvera-Martinez, J. Mendoza-Flores, J. Genesca, *Journal of Loss Prevention in the Process Industries*, 35, pp19–28, 2015.
- [17] 'A review of CO₂ corrosion inhibition by imidazoline-based inhibitor', R.A. Jaal, M.C. Ismail, B. Ariwahjoedi, in: S. Karuppanan, Z.A.A. Karim, M. Ovinis, A.T. Baheta (Eds.) *Icper 2014 – 4th International Conference on Production, Energy and Reliability*, 2014.
- [18] 'Suitability and Stability of 2–Mercaptobenzimidazole as a Corrosion Inhibitor in a Post–

Combustion CO₂ Capture System', L. Zheng, J. Landon, N.C. Koebecke, P. Chandan, K. Liu, *Corrosion*, 71, 6, pp692–702, 2015.

[19] 'Corrosion due to use of CO₂ for enhanced oil recovery', D.W. DeBerry, W.S. Clark, in, U.S. Department of Energy, 1979.

[20] 'Inhibition of steel corrosion under aqueous supercritical CO₂ conditions', Y. Zhang, K. Gao, G. Schmitt, in: CORROSION/2011, NACE International, Houston, TX, USA, Paper No. 11379, 2011.

[21] 'Mn-Mg based zinc phosphate and vanadate for corrosion inhibition of steel pipelines transport of CO₂ rich fluids', M.F. Morks, P.A. Corrigan, I.S. Cole, *International Journal of Greenhouse Gas Control*, 7, pp218–224, 2012.

[22] 'Standard practice for preparing, cleaning, and evaluating corrosion test specimens', ASTM, in: Annual Book of ASTM Standards, G1–03, West Conshohocken, PA, 2003.

[23] 'Standard practice for laboratory immersion corrosion testing of metals', ASTM, in: Annual Book of ASTM Standards, G31, West Conshohocken, PA, 1994.

[24] 'Effect of exposure time on the corrosion rates of X70 Steel in supercritical CO₂/SO₂/O₂/H₂O environments', Y. Xiang, Z. Wang, Z. Li, W. Ni, *Corrosion*, 69, 3, pp251–258, 2013.

[25] 'Long term corrosion of X70 steel and iron in humid supercritical CO₂ with SO₂ and O₂ impurities', Y. Xiang, Z. Wang, Z. Li, W. Ni, *Corrosion Engineering, Science and Technology*, 48, 5, pp395–398, 2013.

[26] 'Corrosion behavior of API 5L X65 Carbon Steel under Supercritical and Liquid CO₂ Phases in the Presence of H₂O and SO₂', F. Farelas, Y.S. Choi, S. Nešić, *Corrosion*, 69, 3, pp243–250, 2013.

[27] 'Formation of ferrous sulfide film from sulfite on steel under anaerobic conditions', T. Hemmingsen, H. Vangdal, T. Valand, *Corrosion*, 48, 6, pp475–481, 1992.

[28] 'Investigation of corrosive effects of sulphur dioxide, oxygen and water vapour on pipeline steels', A.S. Ruhl, A. Kranzmann, *International Journal of Greenhouse Gas Control*, 13, pp9–16, 2013.

[29] 'Raman investigation of iron sulfides under various environmental conditions', I. Weber,

U. Böttger, S.G. Pavlov, H.-W. Hübers, in: 46th Lunar and Planetary Science Conference, The Woodlands, TX, USA, 2015.

[30] 'High-pressure (vapor+liquid) equilibrium in binary mixtures of (carbon dioxide+water or acetic acid) at temperatures from 313 to 353 K', A. Bamberger, G. Sieder, G. Maurer, *The Journal of Supercritical Fluids*, 17, 2, pp97–110, 2000.

[31] 'A review of the protection strategies against internal corrosion for the safe transport of supercritical CO₂ via steel pipelines for CCS purposes', S. Sim, I.S. Cole, Y.S. Choi, N. Birbilis, *International Journal of Greenhouse Gas Control*, 29, pp185–199, 2014.